CROATICA CHEMICA ACTA CCACAA **71** (4) 853–872 (1998)

ISSN-0011-1643
CCA-2535 *Original Scientific Paper*

Ultrafine Zinc and Nickel, Palladium, Silver Coated Zinc Particles Used for Reductive Dehalogenation of Chlorinated Ethylenes in Aqueous Solution

*Weifeng Li and Kenneth J. Klabunde**

Department of Chemistry, Willard Hall, Kansas State University, Manhattan, KS 66506, USA

Received December 10, 1997; accepted May 30, 1998

Zero-valent zinc metal has been employed for the reductive dehalogenation of chlorinated ethylenes. In order to enhance this environmental remediation chemistry, ultrafine zinc particles and transition metal additives (coatings) have been employed. Indeed, activated zinc (cryozinc) significantly enhanced the reduction/dehalogenation process, especially in the presence of nickel and palladium coatings. These reagents were able to achieve rapid, deep reductive dehalogenation of trichloroethylene, trichloroethane, and dichloroethylenes at room temperature under neutral pH conditions. Highest reactivity was found for ultrafine Zn coated with small amounts of palladium. Products, reaction rates, and possible reaction mechanisms and intermediates are presented.

INTRODUCTION

Background

In the past few decades, groundwater has been continually polluted by the widespread use of many chlorinated hydrocarbons. Some of the persistent contaminants, such as trichloroethylene (TCE), tetrachloroethylene

---

This article is dedicated to Professor Egon Matijević on the occasion of his 75th birthday.

* Author to whom correspondence should be addressed.

(perchloro-, PCE), carbon tetrachloride (CT), chloroform (CF) and others, have been used as excellent organic solvents or common degreasing agents at industrial sites throughout the world. Improper disposal practices, leaking storage tanks, accidental spills or other factors have exacerbated ground water pollution by these compounds. Considerable efforts have been made to find ways of reducing theses contaminants. Recent approaches have been photocatalytic oxidation,[1a,b] ultrasound,[1c] pulse radiolysis,[2] microwave plasma discharge,[3] activated carbon adsorption,[4] biochemical transformation,[5] *etc*. Another interesting approach is Metal Enhanced Reductive Dehalogenation technology, which has given positive results in both laboratory and field studies.[6,7]

Since we and others have been interested in metal particle chemistry and catalysis for some time,[8] these reports stimulated considerable excitement, and led to some initial studies of CCl_4 reductive degradation with Mg, Zn, and Sn.[9a] The goal of our work has been to develop reducing systems capable of complete dehalogenation of halogenated organics at room temperature in aqueous solution. As a step towards this goal the work herein was performed, and we have chosen trichloroethylene (TCE), 1,1,2-trichloroethane (TCA), and dichloroethylene (DCE) as chlorocompounds.

Choice of Metals

Thermodynamic considerations suggest that Al, Mg, Sn, Zn, and several first row transition elements are promising for chlorocarbon reduction in water. Indeed, Al and Mg have quite favorable metal halide heats of formation, but likewise very favorable metal hydroxide $\Delta_f H°$. This chemistry is only successful if M^0-chlorocarbon reaction rates are comparative with M^0-H_2O reaction rates. Unfortunately, fine particles of Mg react much too fast with H_2O to be useful, and Al (although further studies are needed) has the same tendency.

Iron and tin also show promise, however they have less reducing power than zinc for lightly chlorinated compounds. Thus, Zn, possessing good reducing potential and competitive reaction rates with chlorocarbons *versus* H_2O, appears to be the most promising. Indeed, we have compared Mg, Al, Fe, Sn, and Zn metals as reductants, and zinc was found to give the fastest, deepest reductive dehalogenation chemistry, and so we centered our efforts on Zn and Ni, Pd, Ag enhanced zinc systems.[9b]

The reaction of interest herein is the complete dehalogenation of trichloroethylene (TCE), and a thermochemical reaction (298 K) can be written as follows:

$$6Zn(s) + 2C_2HCl_3 + 6H_2O \rightarrow$$
$$\rightarrow 3Zn^{2+}(aq) + 6Cl^{-}(aq) + 3Zn(OH)_2(s) + 2C_2H_4(g) \quad (1)$$

$$\Delta H_{rxn} = -1484 \text{ kJ}$$

$$Zn + 2H_2O \rightarrow Zn(OH)_2(s) + H_2 \quad (2)$$

$$\Delta H^{\circ}_{rxn} = -70.4 \text{ kJ}$$

Since this chemistry is dependent on the consumption of Zn(s), it will be sensitive to surface area and cleanliness of the metal. Therefore, ultrafine particles should be of great utility.[9c] Herein we report on the use of commercially available Zn dust, ultrafine particles of Zn prepared by the metal vapor condensation method, and Ni, Pd, and Ag coated Zn particles, to reduce several chlorinated alkenes and an alkane.

EXPERIMENTAL

Reagents and Gases

TCE (anhydrous > 99%, Aldrich Chemical, spectrophotometric grade); Zinc (dust, Aldrich Chemical < 10 micron); Sodium tetrachloropalladium(II) (powder, Aldrich Chemical, ACS grade); Nickel(II) chloride (crystal, Fisher Scientific, ACS grade); Silver nitrate (crystal, Fisher Scientific, ACS grade); Hydrogen (Brown Welding Supply Inc., ultra-pure carrier grade); 1,1,2-TCA (98%, Aldrich, ACS grade); 1,1-DCE (99%, Aldrich); *trans*-DCE (98%, Aldrich); *cis*-DCE (97%, Aldrich); Vinyl chloride (200 μg/ml in methanol, Supelco Inc.); Ethylene (99.5%, Scott II Analyzed Gases, Alltech Associates); Ethane (99%, Scott Specialty Gases); Methyl chloride (> 99.5%, Scott); Ethyl chloride (99.7%, Scott); Acetylene (1% in nitrogen, Scott); Compressed air (UHP/Zero grade, Lineweld Inc., UN 1002).

Apparatus and Procedure

Distilled water was pretreated by bubbling argon gas through it for several hours or overnight, while other chemicals were used without further purification.

Moles (0.115) of metal (weighed to the nearest milligram) and 150.0 ml distilled water were transferred into a 250 ml round bottom flask, the openings were immediately sealed with silicon rubber septa. Using a gas-tight (Hamilton Co.) syringe, 36.7 ml TCE was injected into the liquid phase. The mixture was then agitated by a magnetic stirring bar and stored at room temperature. To insulate the mixture from the heat generated by constant stirring, a piece of styrofoam sheet was placed between the stirrer and the flask. To avoid oxygen contact, it was necessary to set up the apparatus in the hood under Ar flow.

For chloroethylene analysis, 0.196 g (0.003 mol) Zn and 5.0 ml argon saturated H_2O were delivered into a 22 ml glass vial, creating an actual headspace of 16.6 ml. The opening was immediately sealed with a Teflon-faced silicone septum, and crimped with an open-hole aluminum cap. Subsequently, the desired volume of the chlorocarbon was injected into the solvent (water) through a gas-tight syringe. The vials were then rotated on a platform shaker operating at 60 rpm at room temperature.

Analytical Methods

Gas Chromatographic Studies

50 μl of the gaseous phase was collected with a 1 ml pressure-lock syringe (Hamiliton Co.) after a certain period of time, and analyzed by GC (Gow-Mac Instrument Co., series 580) equipped with a thermal conductivity detector. The separation column was 10% SE-30 on Chromosorb W-HP, 80/100 mesh, 12' × 0.125" S.S. (Alltech Associates, Inc.). The column and injector temperature were controlled at 60 and 180 °C, respectively. The detector temperature was set at 200 °C and detector current maintained at 200 mA. Carrier gas was helium at 40 ml/min, approximately twice the optimum linear velocity. Argon or hydrogen gases were directly acquired from the gas cylinders, and the flows set and regulated by orifice flow meters. Carbosphere column and Chemipack C18 column (both 80/100 mesh, 6' × 0.125" S.S., Alltech) were also used to detect other potential decomposition products: ethane, ethene, CO, CO_2 *etc.*

Kinetic aspects of 1,1,2-trichloroethane depletion were studied in 40 ml wheaton bottles, sealed with mininvert valve for convenient syringe withdrawal. Gas phase TCA concentrations were determined at a column temperature of 50 °C with a 5% SE-30 packed column (Alltech), by relating the chromatographic responses in terms of peak area. The carrier gas was helium at a flow of 30 ml/min. The temperatures of injector and detector were 160 and 180 °C, respectively.

Advanced GC Analyses

At appropriate time intervals, the 22 ml serum vials were taken to a Genesis Headspace AutoSampler (Varian Analytical Instruments), and loaded onto a carrousel plate, 50 μl vaporized phase was sampled at a depth of 30% of the vial, and automatically withdrawn by a 100 μl syringe. Injection speed was 2 μl/s with a 6-second needle residence time. Thereafter, the extract was transferred into a GasPro GSC capillary column (30 m length, 0.32 mm i.d., Alltech), and analyzed by GC (Varian Associates, Star 3600CX). The temperature ramp was 36 °C for 3 min, increased at 25 °C/min to 240 °C, and held at the final temperature for 8 min. The injection port and detector temperature were controlled at 200 °C and 300 °C. Helium flow was 40 ml/min with a 50:1 split ratio, and a lower linear velocity might help when extra resolution was needed.

Of the available detection choices, a thermal conductivity detector (TCD) could produce signals for nearly all the molecules, but its sensitivity was about 50 times lower than that of a flame ionization detector (FID). For combustible gases, the FID could generate quantitative results even at trace levels, and was insensitive to minor changes in flow rate, column temperature, or trace amounts of oxygen and water. Therefore, FID became the first choice for chlorocarbon analysis, despite the fact

it could not detect fixed gases (*i.e.,* air, CO_2). In our studies, the inlet pressures of detector gases were controlled at 40 psig for H_2 and 80 psig for air.

pH Change and [Cl^-] Measurements

A portable pH/ISE meter (Orion Research Inc., Model 290A) along with a double junction reference electrode was used. Multipoint pH calibration was performed with the 4.00, 7.00 and 10.00 commercial buffers, where the correct slope should be ±3%. The pH change can also be measured by transferring a few drops of reaction solutions to strips of pH indicator paper.

The same apparatus was also used for [Cl^-] measurements; 3.55, 35.45 and 354.5 ppm standard NaCl solutions were prepared to calibrate the Ag/AgCl electrode. The meter was adjusted to the concentration of the standard. For sample analysis, ionic strength was adjusted with 5 M $NaNO_3$ to 0.1 M.

FT-IR Spectroscopy

Gaseous products were also identified by IR transmission spectra with a Fourier Transform Infrared spectrometer (Bio-Rad Digilab Division, FTS-40). A specific IR gas cell (55 ml volume) was evacuated on the vacuum line, then a background scan was taken. 20 ml of reaction headspace gases was collected into the cell, and its spectrum compared with Sadtler Standard IR Spectra.

XRD Analysis

The reaction solution was filtered through a Buchner funnel under an argon flow, then the solid was dehydrated in the drying cabinet overnight. The collected powder was analyzed by an XDS-2000 scanning diffractometer (Scintag Inc.) using Cu-Kα radiation. The scanning rate was 2°/min from 20 to 80° with a 40 kV tube voltage and 40 mA current.

Gas Chromatographic/Mass Spectrometric Analysis

One gram of Zn and 25 ml Ar purged water were used as the starting materials and delivered into a 40 ml glass serum vial, and 6.6 μl TCE (2.9×10^{-3} M) was injected into the liquid phase through a gas-tight syringe. Sealed with the mininert valves, the wheaton bottles were placed on an M71700 variable speed rotator (Barnstead/Thermolyne Co.) at 60 rpm and kept at room temperature.

Each time just before injection, the glass vials were shaken by hand to equilibrate the gaseous and aqueous phase. Then 1 μl solution was extracted and analyzed by GC-MS (Perkin Elmer Co., Auto System GC/Q-Mass 910) using selected ion monitoring (SIM) scan acquisition. The SIM can monitor up to five different groups of ions with up to 20 selected ions in each group.

A Restek RTx-502.2 (crossbond phenymethyl polysiloxane) capillary column (Alltech Associates, Inc.) was installed with the carrier gas pressure at 27.5 psig. Normal injection was the splitless mode for trace level analysis, when most of the sample entered the column. A multi-ramp temperature program was featured with oven temperature starting from 40 °C to 135 °C at 2 °C/min. Detector and injector temperature were controlled at 180 °C and 200 °C respectively.

BET Analyses

Surface area of the metallic particles was measured by the Brunauer, Emmett, and Teller method, using nitrogen adsorption and helium as the carrier gas. A U-shaped glass tube holding the sample powder was weighed, then attached to the instrument (Micrometrics Flowsorb II 2300). At atmospheric pressure and liquid N_2 temperature, a monolayer of the adsorbate gas was evenly formed on the sample surface. The surface area could be determined by the number of adsorbed molecules.

Metal Samples Employed

Zn Dust

Commercially available Zn dust particle size less than 10 micron was employed. The surface area was 0.3 m^2/g.

Cryo Zinc

This material was prepared by vaporization of Zn metal in a metal vapor reactor, and condensing at 77 K with pentane vapor.[8a–d,9a] Upon warming an ultrafine Zn powder is obtained with surface area = 4 m^2/g.

Ag, Ni and Pd Doped Zinc

Either Zn dust or cryo zinc was treated in water with $AgNO_3$ (aq), $NiCl_2$ (aq), or Na_2PdCl_4 (aq). The aqueous metal salts were reduced by the Zn, yielding a surface coating of Ag^0, Ni^0, or Pd^0. Loadings of these metals were usually 1% (mole fraction, *x*) *vs.* 1 mol Zn. Surface areas were 4, 6, 7 m^2/g for doped Zn and 8, 11, 13 m^2/g for doped cryo Zn.

RESULTS

Reactions of Trichloroethylene (TCE)

pH and Chloride Ion Studies

Experiments employing pure water and zinc with and without TCE were carried out at room temperature. With 0.015 mol Zn dust in 25 ml water, the pH rose from 7.5 to 9 over a period of 50 minutes and then slowly increased to 9.2 over 250 minutes. In the presence of TCE (2.94 mmol), a similar profile was obtained except about 0.5 pH units lower; a rise to 8.5 over 50 minutes, and then to 8.8 over 250 minutes. Actually, the rate of change was sensitive to TCE concentration, as shown in Figure 1, where smaller concentrations kept the pH below 9, but larger concentrations led to even more basic solutions. If reaction (1) is correct, it would be expected that Zn^{2+} and $Zn(OH)_2$ would be formed, and the two together would tend to buffer the solution. Reaction (2), on the other hand, would generate $Zn(OH)_2$ and a pH increase. So the data are understandable, except at high TCE concentra-

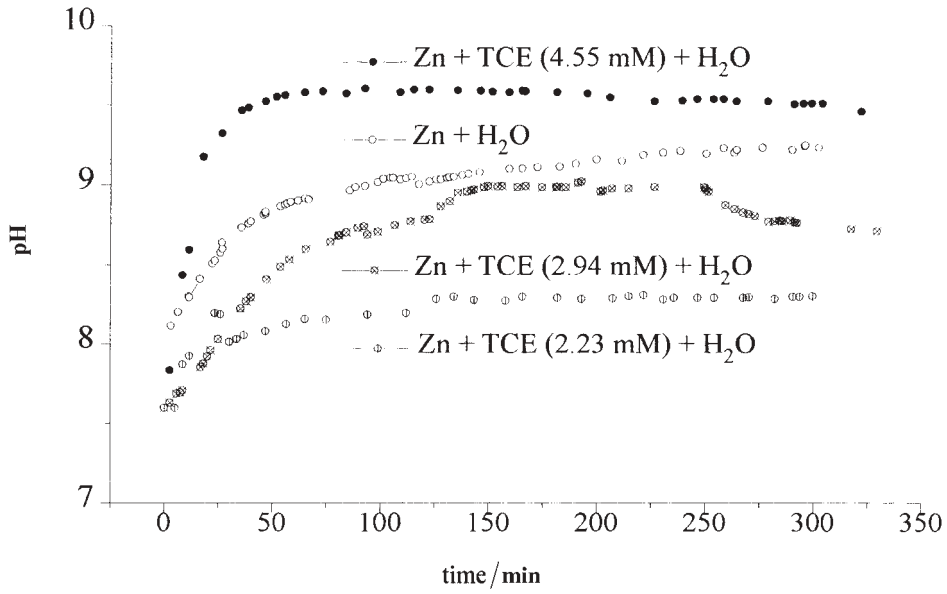

Figure 1. pH changes in the Zn/TCE/H_2O system; effect of TCE concentration.

tions, and suggest that at high concentrations, reaction with the Zn occurs rapidly so that the surface is cleaned, allowing reaction (2) to also proceed more rapidly in the earlier part of the reaction.

In all cases it should be noted that pH never rose above about 9.5, and this is consistent with inhibition of reaction (2) at pH values above 8.[10]

When Ni, Pd, and Ag doping was employed, the TCE reduction rate was greatly enhanced (see later discussion), and pH quickly rose to about 7.5 and then leveled off at 7.0–7.3 over 150 minutes. It appears that reaction (1) dominates in the Ni, Pd, Ag doped systems and the solution is self-buffering.

As expected, chloride ion concentration went up over time, and Figure 2 demonstrates this *versus* TCE concentration decreases.

TCE Degradation

(i) Reaction rates

Infrared spectroscopic studies of the headspace above the Zn/TCE/H_2O reaction mixtures (after 24 hours reaction time) clearly showed the disappearance of TCE and the appearance of saturated and unsaturated hydrocarbons (Figure 3). Note that with Ni and Pd doping, TCE disappearance was complete, and in the case of Pd, strong aliphatic ν_{C-H} appeared. An-

other interesting finding was the formation of CO in the Ag/Zn system, which was only observed where silver was used, and might be due to the use of $AgNO_3$ as the precursor. Currently we have no good explanation for this CO appearance.

Further studies of the headspace gases were carried out by gas chromatography. Volatile organics were readily separated. In order to use the data to determine overall amounts present, a series of standard samples was prepared using pure chlorocarbons, and determining GC peak areas for headspace analyses. A series of calibration curves were constructed. As expected, the less volatile compounds had lower headspace concentrations, while more volatile ones had higher. However, the calibration curves allowed at least good estimates of the total amounts of each component in the reaction mixtures.

Since repeated headspace analyses from one reaction vial would cause outgassing of the water solutions, and complicate the analyses, each reaction vial was analyzed only once (one headspace aliquot). In this way good precision was obtained in our measurements, and a kinetic model of TCE degradation could be developed.

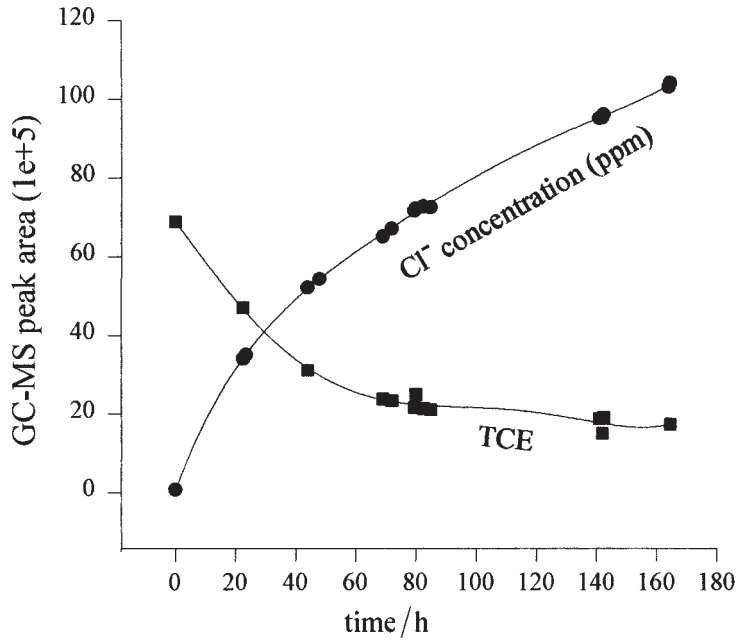

Figure 2. Concentration profile for TCE disappearance and Cl^- accumulation in the $Zn/TCE/H_2O$ system.

The relationship of $\ln(c/c_0)$ (for TCE) *vs.* time was linear over several hours of reaction time, suggesting a first-order TCE degradation rate. The correlated half-lives and rate constants were calculated and summarized in Table I for several of the Zn samples studied. The table is arranged by reaction rate.

It is evident that normal Zn dust is 5 times slower than cryo zinc. When Ag, then Ni, then Pd, are employed as dopants, reactivities are enhanced further and further. In each case the use of a H_2 atmosphere is also beneficial to a moderate degree.

Note that by using Pd doped cryo zinc plus H_2, the rate constant for TCE disappearance is enhanced by a factor of 30 *vs*. cryo zinc, and compared with normal Zn powder, by a factor of nearly 150. Ni and Ag are also effective, but Pd is truly the »champion.«

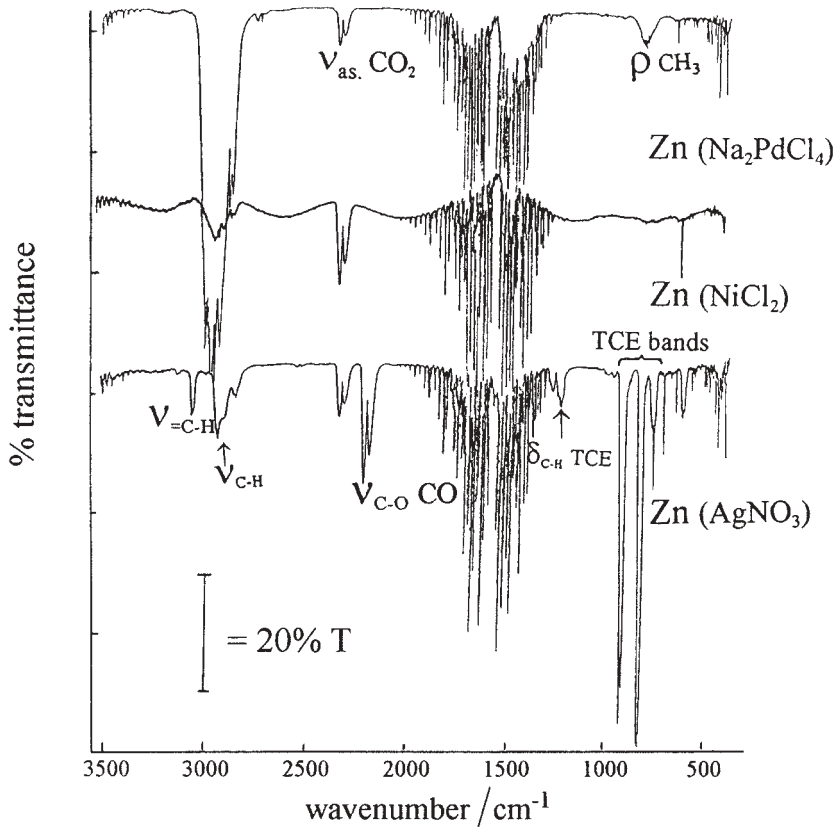

Figure 3. Infrared spectra of the headspace gases in Ag, Ni and Pd doped Zn/TCE/H_2O system after 24 hour reaction time.

TABLE I

Pseudo first-order rate constants and half-lives for TCE degradation over various Zn and Pd, Ni, Ag doped Zn samples, including H_2 and Ar atmosphere

Metallic systems	Specific surface area of zinc $m^2\ g^{-1}$	Surface area concentration $m^2\ dm^{-3}$	$t_{1/2}$ h	k_{obs} h^{-1}
cryo-Zn + Na_2PdCl_4 + H_2	3.90	156	0.69	1.00
cryo-Zn + $NiCl_2$ + H_2	3.90	156	1.9	0.37
cryo-Zn + Na_2PdCl_4	3.90	156	4.5	0.16
cryo-Zn + $NiCl_2$	3.90	156	7.2	0.097
cryo-Zn + $AgNO_3$ + H_2	3.90	156	8.6	0.080
cryo-Zn + $AgNO_3$	3.90	156	14	0.048
cryo-Zn + H_2	3.90	156	15	0.046
cryo-Zn	3.90	156	22	0.032
Zn + H_2	0.27	10.8	76	0.009
Zn	0.27	10.8	95	0.007

Products observed were *cis*- and *trans*-1,2-dichloroethylene (DCE), 1,1-DCE, vinyl chloride (VC), acetylene, ethylene, and in some cases small amounts of CH_2Cl_2 and CH_3Cl. The steps leading to formation of all these products are discussed later.

(ii) Effect on remaining zinc

Interestingly, metal surface areas/g increased during reaction with the TCE/H_2O system, which is demonstrated by Figure 4. Thus, cryo Zn started with a surface area of 4 m^2/g, increased to 6 m^2/g after 24 hours of reaction with TCE/H_2O, but to 7 m^2/g after 24 hours with cryo Zn/Ag, 10 m^2/g with cryo Zn/Ni, and all the way up to 13 m^2/g after 24 hours of reaction with cryo Zn/Pd. These data clearly show that erosion and consumption of Zn take place in such a way that more porous Zn with higher surface area is continually formed. This has been confirmed by atomic force microscopy (AFM)[11] studies showing that columnar structures are formed, and an example is shown in Figure 5.

These results are considered welcome in the sense that reactivity of the Zn, based on its higher specific surface area, should increase over time (until, of course, the Zn is all consumed).

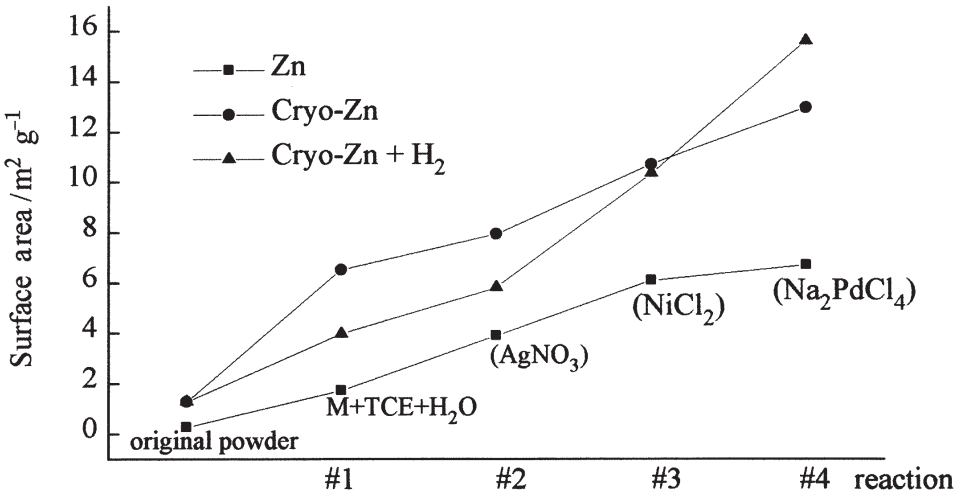

Figure 4. Surface area of metallic Zn particles before and after 24 hour of reaction with TCE/H_2O; each point is a 24 hour reaction time.

(iii) Solid products

After extensive reaction, the remaining water, TCE and volatile products were removed by filtration, and the solid residue studied by powder X-ray diffraction (XRD). Figure 6 shows that besides remaining metallic Zn, ZnO was the main solid product, along with some $Zn(OH)_2$ and $ZnCl_2$ (most of the $ZnCl_2$, being soluble in water, would have remained in the water solution.) Indeed, by evaporation of the water from the aqueous solutions, and XRD analysis of the solid residue, it was shown that $ZnCl_2$ and its hydrate were the major components. These data again clearly point out the enhanced reactivity of the Ni and Pd doped samples.

Reactions of 1,1,2-Trichloroethane (TCA)

Since the IR data suggested that saturated hydrochlorocarbons were formed as intermediates in the Zn reduction/dechlorination of TCE, it was deemed necessary to compare TCA in reactivity.

Data were collected using Zn dust, and Ni and Pd promoted Zn dust. These data points were fitted to a two-parameter exponential decay model, and pseudo first-order rate constants k_{obs} / h determined as 2.8 (Zn dust), 4.4 (Zn/Ni), and 7.6 (Zn/Pd). These rates are remarkably high compared

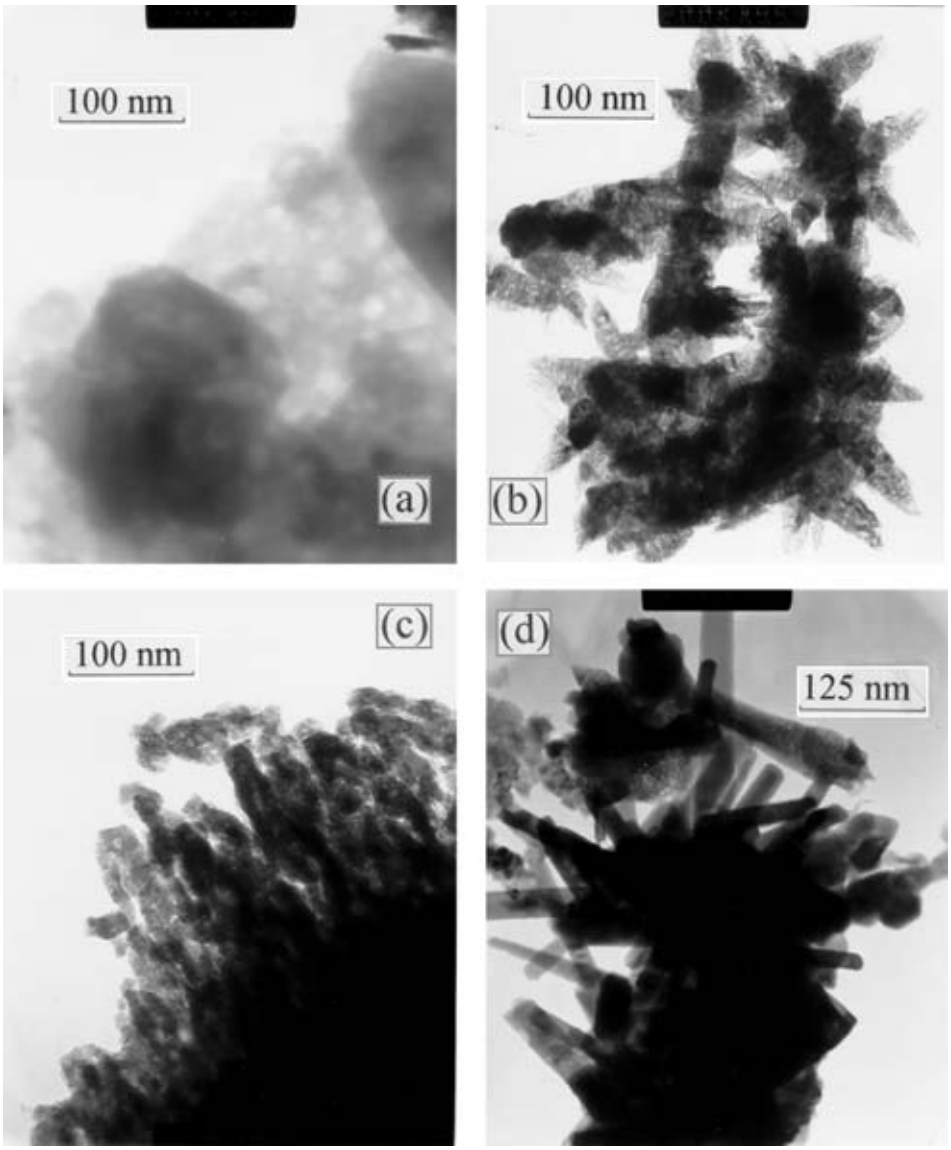

Figure 5. Transmission electron microscopy (TEM) studies of Zn corrosion; (a) cryo Zn before reaction, (b) cryo Zn/Pd before reaction, (c) cryo Zn/Pd after 24 hours of exposure to pure water, (d) cryo Zn/Pd after 24 hours of exposure to TCE/H_2O solution.

with those for TCE (Table I); for example with Zn dust alone k_{obs} = 0.007 (TCE) and 2.8 (TCA). Obviously, TCA is much more rapidly degraded than TCE.

Reactions of cis- *and* trans-*1,2-Dichloroethylene (DCE) and 1,1-DCE*

Since DCE was found to be a relatively persistent product in the degradation of TCE, some kinetic data for starting DCE was obtained. Once again the presence of Ni and Pd caused a great enhancement in degradation rates; however, all three DCE isomers reacted with similar rates, and their disappearance was slower than TCE and much slower than TCA.

Total Product Analyses

A broad series of experiments were carried out where cryo Zn, cryo Zn/Ni, cryo Zn/Pd, Zn (dust), Zn/Ni, and Zn/Pd were allowed to react with TCA, TCE, 1,1-DCE, *cis*-DCE, and *trans*-DCE. All products in the vapor phase were analyzed in terms of extents of conversion to products of the starting materials.

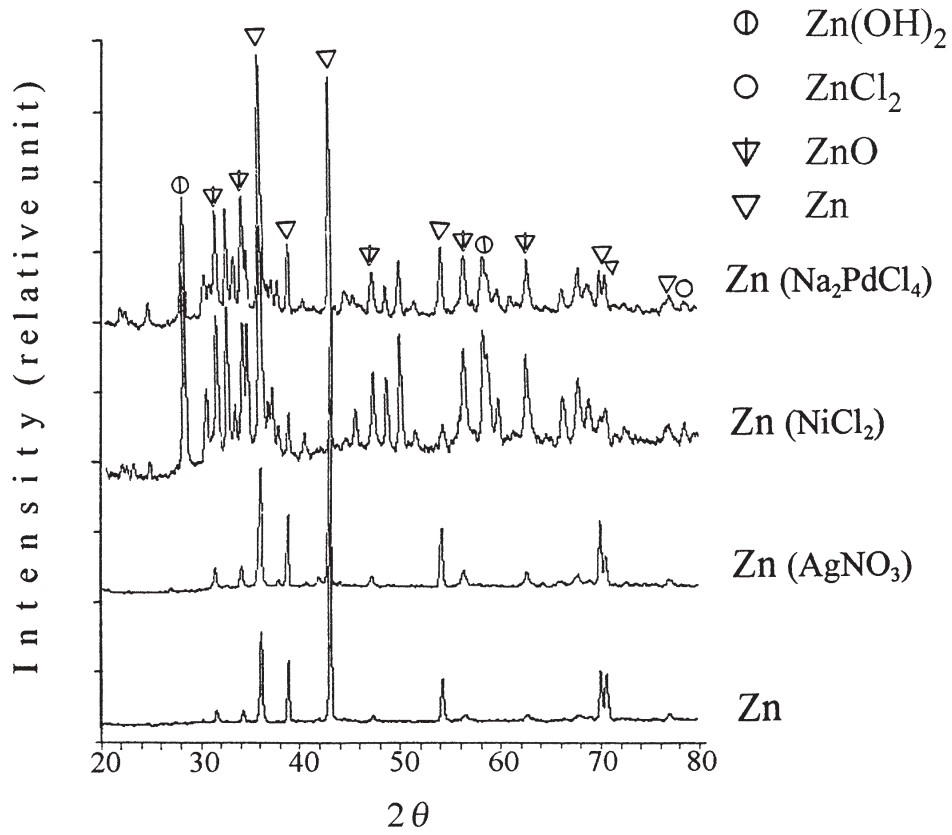

Figure 6. XRD spectra of solid products of Zn TCE/H_2O reactions.

As expected, the cryo-Zn systems caused much faster degradation/reduction of all the starting materials. However, the addition of Ni or Pd caused greatly enhanced reactivities, and tended to level out differences between the cryo samples and normal Zn dust.

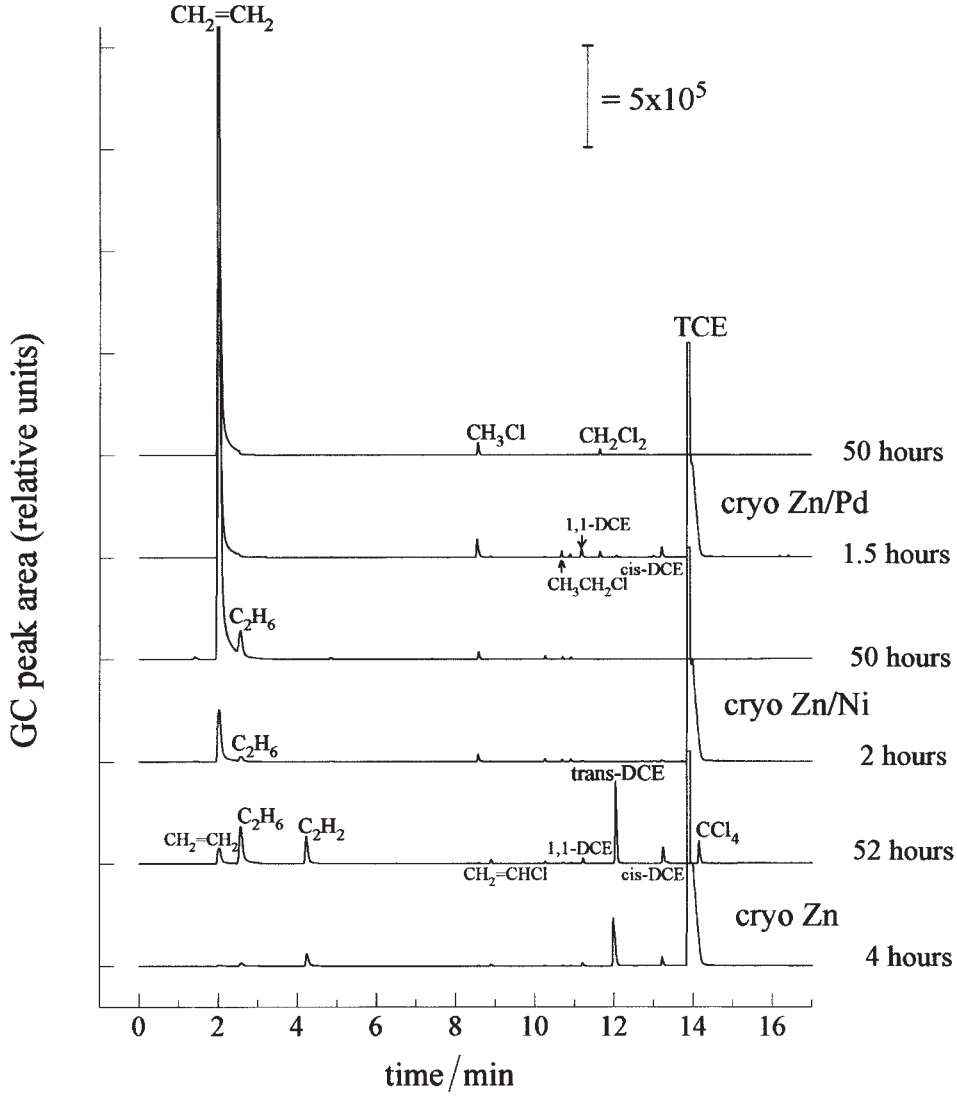

Figure 7. Gas chromatographs of products from TCE degradation by cryo Zn and Ni or Pd doped cryo Zn.

Figure 7 illustrates the GC data for cryo Zn and doped cryo Zn samples for TCE degradation. Note the comparatively rapid and almost complete conversion to ethylene by the cryo Zn/Pd sample.

Another type of representation is shown in Figure 8, where Zn dust and doped Zn dust – TCE data are shown in bar graph form. Note that it takes

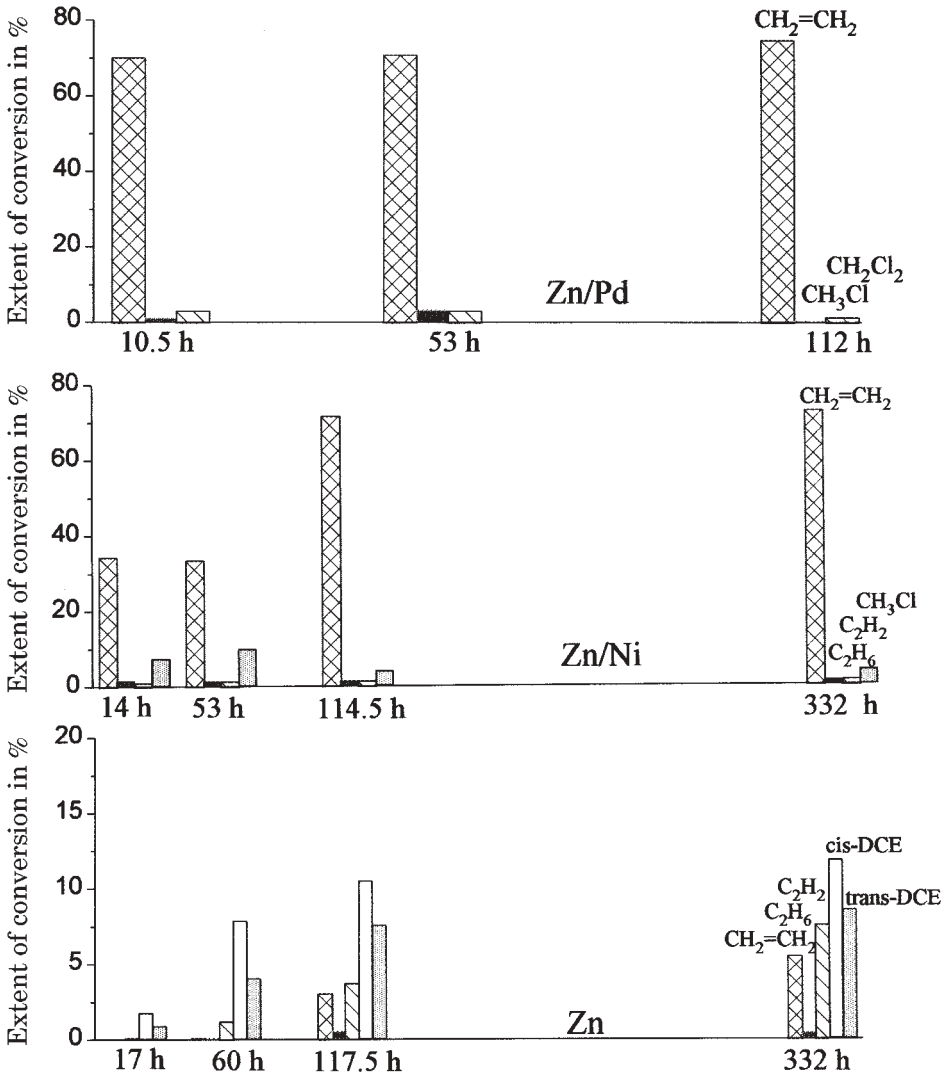

Figure 8. Product distributions in the TCE degradation by Zn dust, and Ni and Pd doped Zn dust; mole fractions (x) of starting material converted.

about 17 hours before any significant production of products occurs with Zn dust, and even after 332 hours considerable amounts of DCE remain. However, the presence of Ni, and especially Pd causes dramatic differences to that ethylene is dominant after 10 hours of reaction time.

Table II shows typical data for these studies and illustrates the cryo Zn/Ni system. Note the reasonably high mole fraction converted to ethylene at the longer (50 hour) reaction times.

DISCUSSION

In all the direct comparisons, TCA was always degraded considerably faster than TCE. Coupled with the fact that: (1) saturated compounds appeared to be intermediates during IR monitoring; (2) a H_2 atmosphere accelerates degradation rate, and; (3) Pd, a good hydrogenation catalyst, is the best doping agent, it seems likely that one degradation pathway involves hydrogenation, dehydrohalogenation (Scheme 1, path 1). However, earlier

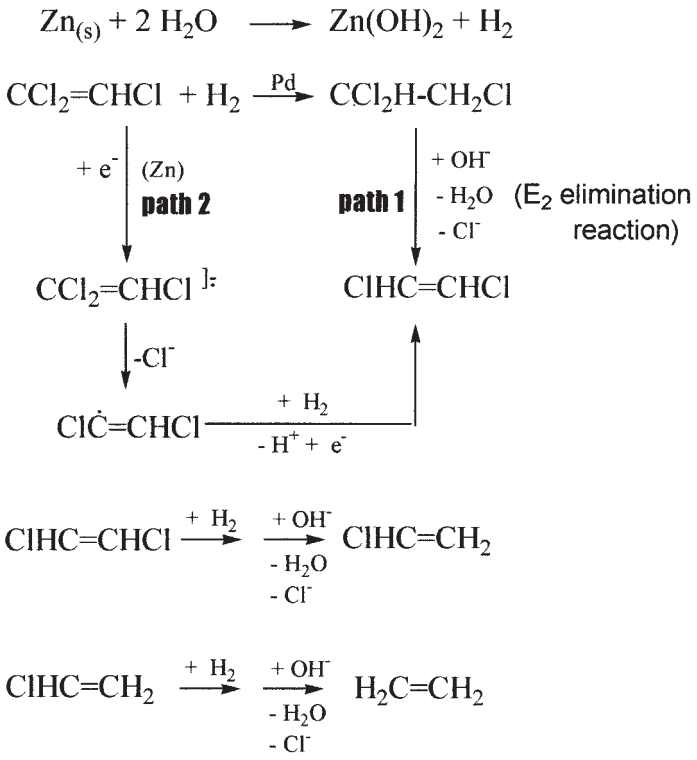

Scheme 1. Proposed reaction pathways for reduction of TCE by Zn/Pd.

TABLE II

Product distribution in the cryo Zn/Ni degradation in mole fractions expressed in % with respect to TCE converted

Starting Material	Time h	$CH_2=CH_2$	$CH_3–CH_3$	$CH_2=CHCl$	CH_3CH_2Cl	CH_3Cl	TCA	TCE	1,1-DCE	*cis*-DCE	*trans*-DCE
TCA	1.25	7.1	0.90	1.4	–	–	59	–	–	–	–
	49.5	73	0.24	–	–	–	–	–	–	–	–
TCE	2	15	0.84	–	–	0.85	–	76	–	–	–
	50	72	0.92	–	–	1.2	–	–	–	–	–
1,1-DCE	1.75	8.6	2.0	–	–	–	–	–	85	–	–
	51	66	3.1	–	–	–	–	–	–	–	–
cis-DCE	2.5	40	8.2	0.40	2.6	4.4	–	–	0.64	26	–
	50	71	2.6	–	1.1	3.8	–	–	–	–	–
trans-DCE	3	13	2.6	–	3.4	5.3	–	–	0.68	–	–
	50.5	70	–	–	1.4	3.4	–	–	0.28	–	0.25

work has shown that Pd also greatly enhances degradation/reduction of CCl_4, $CHCl_3$, CH_2Cl_2, and CH_3Cl, and electron transfer appeared to be rate determining.[9,11] Therefore, path 2 in Scheme 1 probably competes with path 1.

Besides the major products of DCE and ethylene, some unexpected trace products were found, including ethane, acetylene, CH_2Cl_2, and CH_3Cl. Ethane can be explained as a hydrogenation product of ethylene, and acetylene from dehydrohalogenation of vinyl chloride. The monocarbon species are more puzzling, and may indicate the presence of intermediate organometallic species on the surface of the Zn/Pd surface.

Indeed, all of the products could be explained by involving transient organometallics, as we have proposed earlier for Zn-CCl_4/H_2O reduction chemistry.[9,11] Scheme 2 illustrates two possible pathways that could occur on the surface. Since more CH_3Cl and CH_2Cl_2 were generally observed when Ni or Pd was present, it seems possible that C=C cleavage on these transition metal surfaces occurs. However, these represent only a few of the possible reaction pathways that may actually take place in this complex, rather unexplored chemistry. There is certainly a need for more careful studies of mechanistic features.

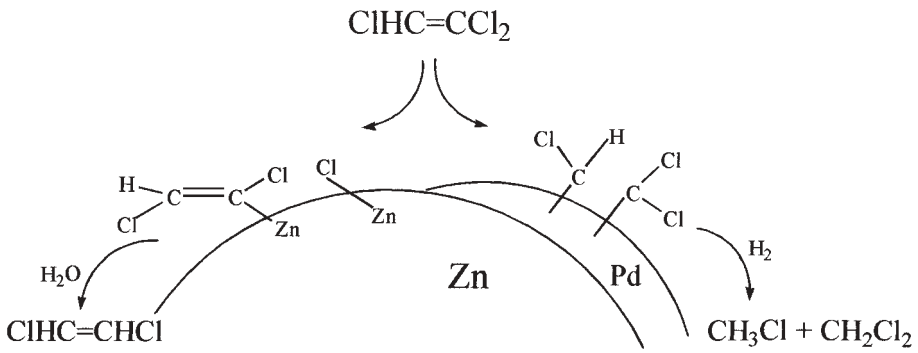

Scheme 2. Proposed organometallic surface intermediates involved in TCE reduction by Zn/Pd.

CONCLUSIONS

The results show that the high surface area cryo Zn is much more reactive than normal Zn powder, a finding that is not unexpected. Furthermore, the presence of Ni, Pd, or Ag greatly enhances the degradation so that deep reduction occurs quickly, and this is especially the case with cryo Zn/Ni and cryo Zn/Pd. This can be attributed to several factors: (1) greater surface areas;

(2) cleaner, more reactive surface sites; (3) the resistance of Ni, Pd, or Ag to corrosion (relative to Zn, which is consumed and converted to $ZnCl_2$ (aq) and $Zn(OH)_2$ (s), thereby allowing continued ability to allow electron transfer chemistry at the surface even as Zn is being corroded and consumed.

Thus, it is clear that ultrafine metal powders offer considerable advantages in this interesting area of environmental remediation chemistry.

Acknowledgements. – The support of the Army Research Office, and the Hazardous Substance Research Center at Kansas State University is acknowledged with gratitude.

REFERENCES

1. (a) L. A. Dibble and G. B. Raupp, *Catal. Lett* **4** (1990) 345–354.
   (b) L. A. Dibble and G. B. Raupp, *Environ. Sci. Technol.* **26** (1992) 492–495.
   (c) C. Petrier, M. Micolle, G. Merlin, J. Luche, and G. Reverdy, *Environ. Sci. Technol.* **26** (1992) 1639–1642.
2. (a) Y. Tabata, *Pulse Radiolysis* **1**, CRC, Boca Raton, 1991.
   (b) R. Mertens, C. V. Sonntag, J. Lind, and G. Merenyi, *Angew. Chem., Int. Ed. Engl.* **33** (1994) 1259–1261.
3. K. W. Yost, 43rd Prude Industiral Waste Conference Proceedings, p. 441.
4. P. H. Chen, C. H. Jenq, and K. M. Chen, *Environ. Inter.* **22** (1996) 343–359.
5. (a) T. J. Phelps, J. J. Niedzielski, R. M. Schram, S. E. Herbes, and D. C. White, *Appl. Environ. Microbiol.* **56** (1990) 1702–1709.
   (b) R. G. Zytner, *Water Air Soil Pollut.* **65** (1992) 245–255.
   (c) T. M. Vogel and P. L. McCarty, *Appl. Environ. Microbiol.* **49** (1985) 1080–1083.
   (d) N. H. Back, P. R. Jaffe, and N. Shingal, *J. Environ. Sci. Health* **25** (1990) 987–1005.
6. (a) A. L. Roberts, L. A. Totten, W. A. Arnold, D. R. Burris, and T. J. Campbell, *Environ. Sci. Technol.* **30** (1996) 2654–2659.
   (b) T. Senzaki and Y. Kumagai, *Kogyo Yosui* **369** (1989) 19–25.
   (c) W. S. Orth and R. W. Gillham, *Environ. Sci. Technol.* **30** (1996) 66–71.
   (d) L. J. Matheson and P. G. Tratnyek, *Environ. Sci. Technol.* **28** (1994) 2045–2053.
7. (a) R. W. Gillham, and S. F. O'Hannesin, *Groundwater* **32** (1994) 958–967.
   (b) R. C. Starr and J. A. Cherry, *Groundwater* **32** (1994) 465–476.
   (c) R. W. Gillham and S. F. O'Hannesin, *Groundwater* **29** (1991) 749–756.
8. (a) K. J. Klabunde and T. O. Murdock, *J. Org. Chem.* **44** (1979) 3901–3908.
   (b) K. J. Klabunde, *Free Atoms, Clusters, and Nanoscale Particles*, Academic Press, San Diego 1994.
   (c) K. J. Klabunde, *Chemistry of Free Atoms and Particles*, Academic Press, New York 1980.
   (d) K. J. Klabunde and G. Cardenas, in: A. Fürstner (Ed.), *Active Metals Preparation, Characterization, Application*, VCH Pub., Weinheim 1996, pp. 237–275.
   (e) P. Cintas, *Activated Metals in Organic Synthesis*, CRC Press, Boca Raton, 1993.
   (f) R. D. Rieke, *Acc. Chem. Res.* **10** (1977) 301–306.
9. (a) T. N. Boronina, K. J. Klabunde, and G. Sergeev, *Environ. Sci. Technol.* **29** (1995) 1511–1517 and references therein.

b) Of course any consideration of zinc as the metal of choice must include environmental and cost considerations. However, it is our intent here only to determine what is possible regarding depth of reduction and reaction rates/intermediates. (c) the terms »finely divided« or »ultrafine« are all encompassing. Nanoscale particles, nanocrystals, colloids, and ultrafine particles are generally synonyms in recent literature. Actually, zinc at a surface area of 4 cm^2/g is not as finely divided as transition metals can be produced, which can be in the range of 50 m^2/g in activated form. This is because of the low melting point and ease of analgamation of zinc. However, zinc is highly reactive on a comparative basis. See T. L. Johnson, M. M. Scherer, and P. G. Tratnyek, *Environ. Sci. Technol.* **30** (1996) 2634–2640, for a discussion of surface areas of commercial iron samples, which are generally in the range of 0.1 to 3.3 m^2/g.

10. D. P. Siantar, C. G. Schreier, and M. Reinhard, *Prepr. Pap. ACS Natl. Meet., Am. Chem. Soc., Div. Environ. Chem.* **35** (1995) 745–748.
11. (a) T. N. Boronina, L. Dieken, I. Lagadic and K. J. Klabunde, *J. Hazard. Subst. Res.*, in press.
(b) T. N. Boronina, I. Lagadic, K. J. Klabunde, and G. Sergeev, *Environ. Sci. Technol.* **32** (1998) 2614–2622.

SAŽETAK

Uporaba ultrafinih čestica cinka prekrivenih niklom, paladijem, srebrom i cinkom za reduktivno dehalogeniranje kloriniranih etilena u vodenim otopinama

Weifeng Li i Kenneth J. Klabunde

Elementarni cink obično se rabi za reduktivno dehalogeniranje kloriranih etilena. U cilju poboljšanja toga ekološki važnog procesa, uporabljene su ultrafine čestice cinka s dodatkom (presvlakom) prijelaznih metala. Naravno, aktivirani cink (kriocink) znatno poboljšava procese redukcije/dehalogeniranja, posebno kada je prekriven niklom i paladijem. Ti su reagensi vrlo efikasni za brzo, duboko reduktivno dehalogeniranje trikloroetilena, trikloroetana, i dikloroetilena pri sobnoj temperaturi pri neutralnom pH. Velika reaktivnost opažena je za ultrafini Zn prekriven malom količinom paladija. U radu su prikazani produkti, brzine reakcija, mogući reakcijski mehanizmi i međuprodukti.